Title
AH ANALYSIS OF Kn SCATTERING FROM THE REACTION K+n K+n-p+

Author
Firestone, A.

Publication Date
1971-12-01

Submitted to Physical Review

LBL-516
Preprint c.1

AN ANALYSIS OF Kπ SCATTERING FROM THE REACTION $K^+n \to K^+\pi^-p^+$

A. Firestone, G. Goldhaber, D. Lissauer
and G. H. Trilling

December 1, 1971

AEC Contract No. W-7405-eng-48

DISCLAIMER

LBL-516

AN ANALYSIS OF Kπ SCATTERING FROM THE REACTION $K^+n \to K^+\pi^-p$ †

A. Firestone,* G. Goldhaber, D. Lissauer, and G. H. Trilling

Department of Physics and Lawrence Berkeley Laboratory
University of California, Berkeley, California 94720

December 1, 1971

ABSTRACT

We have analyzed $K^+\pi^-$ elastic scattering in the reaction $K^+n \to K^+\pi^-p$ at 12 GeV/c. We have extrapolated to the pion pole in order to obtain the on-mass-shell $K^+\pi^-$ elastic scattering cross section and angular distributions as functions of Kπ mass in the range from threshold to 2 GeV. Using a simple model of Kπ elastic scattering we have determined solutions of the $I = 1/2$ S-wave phase shift for $m(K\pi) < 1.7$ GeV. We find that the $I = 1/2$ S-wave amplitude performs at least one complete loop in the Argand plot ("down" solution). In addition, if one chooses the appropriate "up" solutions two rapidly varying loops at $m(K\pi)$ near the $K^*(890)$ and $K^*(1420)$ respectively are also allowed by our data.

I. INTRODUCTION

Analyses of $K\pi$ scattering, using one-pion-exchange processes have been discussed in several recent papers. These studies have involved reactions:

$$K^+p \rightarrow (K\pi)^0\Delta^{++}(1236) \quad (1)$$

$$K^-p \rightarrow (K\pi)^-p \quad (2a)$$

$$K^-p \rightarrow (K\pi)^0n \quad (2b)$$

$$K^-n \rightarrow (K\pi)^{--}p \ . \quad (2c)$$

Data from reaction (1) at 7 GeV/c were used by Trippe et al.[1] to determine $K\pi$ elastic cross sections and angular distributions up to masses of 2 GeV.

Recently, more extensive data samples of reaction (1) between 2.5 and 13 GeV/c from the World Data Summary Tape have been used to calculate the S-wave $I = 1/2$ $K\pi$ amplitude between threshold and about 1.1 GeV.[2,3] At the same time, reactions (2) at 5 GeV/c have also been used to extract the S-wave phase shift up to about 1.2 GeV.[4] The recent analyses all indicate two possible $I = 1/2$ S-wave phase shift solutions: (a) a "down" solution with a slowly varying phase shift which rises to about 60-70° at 1 GeV and (b) an "up" solution which contains a relatively narrow resonance at about the same mass as the $K^*(890)$.

In this paper, we report the results of a study of $K^+\pi^-$ scattering from threshold to a $K\pi$ mass of 1.7 GeV, based on a study of the reaction,

$$K^+n \rightarrow K^+\pi^-p \ , \quad (3)$$

at an incident momentum of 12 GeV/c. The data were obtained in a 500,000-picture exposure of the deuterium-filled SLAC 82-inch bubble chamber to a 12-GeV/c rf-separated K^+ beam. The complete analysis of the film has yielded a sample of 6419 $K^+n \rightarrow K^+\pi^-p$ events, which correspond to a cross section of 400 ± 20 μb. The experimental details, as well as some particular aspects

of Kπ scattering seen in these data have been reported previously.[5-8] Reaction (3) is analogous to (2b), but our momentum is much higher than that of Yuta et al.,[4] and our procedure very different.

II. Kπ CROSS SECTIONS

For the study of Kπ scattering, there are several significant differences between reactions (2b), (3) and reaction (1). First of all, the kinematic boundary for the reaction with the nucleon in the final state allows the physical region to approach much closer to the pion pole than it does for the reaction with the delta in the final state. This dramatic difference in the kinematically allowed regions, particularly important at high Kπ masses, is seen in Fig. 1, which shows the kinematic boundaries for the two reactions (1) and (3), each calculated at 12 GeV/c incident momentum. Secondly, the baryon vertex function for the delta reaction is different from that for the reactions with nucleons in the final state. As a consequence of this difference the behavior of the cross sections in the neighborhood of $t = 0$ is different in the two cases.

We assume that, for small enough momentum transfers, the reaction $K^+n \rightarrow K^+\pi^-p$ does in fact proceed primarily through pion exchange. We therefore restrict our attention to the region with $t < 0.2$ $(GeV/c)^2$, where t is the square of the four-momentum transfer from incident neutron to final proton.[9] In this region the Treiman-Yang angular distributions are consistent with isotropy for all values of $m(K^+\pi^-)$. The t-dependence of the data may be represented by an exponential, $d\sigma/dt = Ae^{-Bt}$, where $B \sim 10$ $(GeV/c)^{-2}$ for all regions of $m(K^+\pi^-)$. The Dalitz plot for this reaction has been published previously[7] as has the scatter plot of $\cos\theta$ vs $m(K^+\pi^-)$, where θ is the polar angle in the Gottfried-Jackson frame.[8]

We have followed the procedures of Colton and Malamud[10] and Ma et al.[11] in extrapolating the cross section to the pion pole. The pole equation is given by,[12]

$$\frac{d^2\sigma}{dtdm} = \frac{1}{4\pi m_t^2 p_\ell^2} \left(\frac{g^2}{4\pi}\right) \frac{t}{(t+\mu^2)^2} m^2 q(m) \sigma(m) F(m,t) \quad , \qquad (4)$$

in which m_t is the target (nucleon) mass, p_ℓ is the incident laboratory momentum, $(g^2/4\pi) = 29.2$, μ is the pion mass, m is the $K^+\pi^-$ invariant mass, q(m) is the on-shell momentum in the $K^+\pi^-$ rest frame, $\sigma(m)$ is the on-shell $K^+\pi^-$ elastic cross section, and F(m,t) is a form factor whose value is unity at the pion pole. In Eq. (4) all masses and momenta are in GeV and all cross sections in mb. For the function F(m,t), we make the same choice as Colton and Malamud,[10] namely

$$F(m,t) = G(m,t)\left(\frac{1 + 7.1\, p^2}{1 + 7.1\, p_t^2}\right) \quad , \qquad (5a)$$

$$\text{where} \quad G(m,t) = \left(\frac{2.3 - \mu^2}{2.3 + t}\right)^2 \left(\frac{q_t}{q}\right)^2 \left[\frac{1 + (8.3\, q)^2}{1 + (8.3\, q_t)^2}\right] \quad , \qquad (5b)$$

in which q_t is the momentum of the incident K^+ in the $K^+\pi^-$ rest frame, p_t is the momentum of the incident neutron in the proton rest frame, and p is the value of this momentum at the pion pole; i.e., p^2 is a negative quantity.

The terms involving q, q_t in (5b) have the Dürr-Pilkuhn form[13] corresponding to a P-wave Kπ system. We have however used them even in Kπ mass regions dominated by other waves (S and D). Our justification is that in principle F(m,t) can be any smooth function which goes to unity at the pole, and the usefulness of a particular choice is determined by the ability to extrapolate Eq. (4) from the physical region to the pole with a simple t-dependence. The form (5) did permit a simple linear extrapolation in t throughout the whole Kπ mass range studied; this is taken as <u>a posteriori</u> justification for the form of F(m,t) used. The use of such form factors has been shown[14-16] to describe Chew-Low distributions for reactions of the type $Xp \to X\pi^+n$ (X = π, K or p) for many incident momenta.

We use the expression,[10]

$$\text{"t}\sigma\text{"} = \frac{n}{\int dtdm} \sum_{i=1}^{N} \left[\frac{t}{(d^2\sigma/dtdm)_{OPE}}\right]_i \qquad (6)$$

to evaluate "tσ" for a given $\Delta t \Delta m$ bin, where n is the mb/event ratio in this experiment. The sum is performed over all events in the particular $\Delta t \Delta m$ bin, and the bracketed quantity is calculated individually for each event in the bin. The integral $\int dtdm$ is performed over that portion of the particular $\Delta t \Delta m$ bin which is included in the physical region of the Chew-Low plot. The denominator in brackets in Eq. (6), $(d^2\sigma/dtdm)_{OPE}$, is given by Eq. (4) with $\sigma(m)$ set equal to unity.

The procedure is to fit polynomials in t to the experimental "tσ" points. Least squares fits have been performed separately to the forms "tσ" = bt, "tσ" = a + bt, and "tσ" = a + bt + ct^2. In every case it was found that c did not differ significantly from zero, and that no significant improvement in χ^2 probability was obtained by adding the quadratic term. Therefore we have considered only the linear extrapolations "tσ" = bt and "tσ" = a + bt, which give reasonable χ^2 values in nearly all bins. Figure 2 shows the extrapolation to the pole in each bin in $m(K^+\pi^-)$ for the polynomial "tσ" = a + bt. The results are presented in Table I, and the cross sections for the two extrapolations are plotted in Figs. 3 and 4.

In principle, the quantity "tσ" as defined in Eq. (6) should pass through zero at t = 0. It actually appears from Table I that in a number of $m(K\pi)$ bins, the quantity a, from the fit "tσ" = a + bt, is significantly different from zero. This discrepancy may be attributable to the effects of absorption.[17] On the other hand, the results of the CERN-Brussels-UCLA Group,[3] based on extrapolation of the somewhat different pole equation applicable to reaction (1), agree better with our "tσ" = bt fits than the "tσ" = a + bt fits, particularly

in the neighborhood of the $K^*(890)$. We are therefore unable to make a compelling argument in favor of one form rather than the other.

We observe from Fig. 4 that the cross section $\sigma(K^+\pi^- \to K^+\pi^-)$ is dominated by the $K^*(890)$, and also has a significant enhancement corresponding to the $K^*(1420)$. The width of the $K^*(890)$ peak is consistent with the conventional value of about 50 MeV observed in $K\pi$ mass distributions, but the value of the cross section in the highest bin (0.88 GeV $< m(K^+\pi^-) < 0.92$ GeV) is significantly higher than the P-wave unitarity limit. As is well known this effect is attributable to the presence of a large S-wave phase shift in this region.[18] The peak in the region of the $K^*(1420)$ appears broader than the conventional 100 MeV observed in $K\pi$ mass distributions, and is centered more at 1.35 GeV than at 1.4 GeV. Evidence has been presented previously for an additional resonance on the low-mass side of the $K^*(1420)$.[7] The extrapolated cross section, using either extrapolation procedure, exceeds the calculated D-wave contribution of the $K^*(1420)$, based on an elasticity of 57%. This excess may be due to the presence of a large S-wave phase shift in this mass region.

III. ANGULAR DISTRIBUTIONS

As has been done in previous analyses[16] we express the $K\pi$ angular distributions in terms of the average values of spherical harmonics $\langle Y_\ell^m \rangle$. We have considered two ways of determining these moments, namely (i) by extrapolation to the pole and (ii) by averaging over the physical region in the momentum transfer range $t < 0.2$ $(\text{GeV}/c)^2$.

The extrapolation to the pole was done in the same bins in both t and $m(K\pi)$ used to extrapolate the quantity "$t\sigma$". The procedure was to calculate the average value of the particular spherical harmonic, $\langle Y_\ell^m \rangle$, in each bin $\Delta t \Delta m$, and then to extrapolate the t-dependence of $\langle Y_\ell^m \rangle$ to the pion pole for each value of $m(K\pi)$. This was done separately for each bin in $m(K\pi)$ and for

each particular spherical harmonic. The extrapolation used in each case was linear; i.e., "$\langle Y_\ell^m \rangle$" = a + bt. We found no evidence for a quadratic term in any "$\langle Y_\ell^m \rangle$" distribution in any mass bin. The linear fit gives a reasonable χ^2 in most cases. We have considered only Y_ℓ^o terms with $\ell \leq 4$; consequently our subsequent partial wave analysis applies only up to about $m(K\pi) = 1.7$ GeV.[8] The extrapolated $\langle Y_1^o \rangle$ to $\langle Y_4^o \rangle$ are listed in Table II and shown in Fig. 5. The $\langle Y_\ell^m \rangle$, where $m \neq 0$, are not significantly different from zero.

It has been pointed out by Kane[17] that extrapolations of quantities such as $\langle Y_\ell^m \rangle$ for reactions (2) and (3) may run into singularities before getting to the pion pole. Since this may cast some doubt on the validity of the $\langle Y_\ell^m \rangle$ obtained by extrapolations such as those just described, we have also considered the moments calculated in the physical region, $t \leq 0.2$ (GeV)^2. Values of these moments are given in Table III and shown in Fig. 6. The general features of the extrapolated and physical region $\langle Y_\ell^o \rangle$ are very similar, although the structures tend to be slightly more accentuated in the extrapolated moments. It is interesting to compare our values of $\langle Y_\ell^o \rangle$ with those obtained by extrapolation using data from reaction (1). The vertex functions are different in that reaction, and the criticism of the extrapolation of moments mentioned above does not apply. The moments calculated from reaction (1) are in reasonable agreement with both our physical region moments and with our extrapolated values.[3]

The general qualitative features of the moments are as follows. $\langle Y_1^o \rangle$ is large and falling rapidly near the $K^*(890)$, remains small between 1.0 and 1.4 GeV and then rises again. $\langle Y_2^o \rangle$ has maxima in the neighborhoods of both $K^*(890)$ and $K^*(1420)$ although the latter peak seems to occur at about 1.5 GeV rather than at the conventional D-wave resonance mass. The value of $\langle Y_3^o \rangle$ remains small up to about 1.6 GeV at which point it rises rapidly. Finally $\langle Y_4^o \rangle$ is close to zero up to 1.4 GeV at which point it exhibits significant structure.

IV. PARTIAL WAVE ANALYSIS

We have attempted to fit the cross section and angular distribution data listed in Tables I, II and III to the following simple model of $K^+\pi^-$ elastic scattering. The cross sections and moments are given by the following equations:

$$\sigma = 4\pi\lambda^2\{|S|^2 + 3|P|^2 + 5|D|^2\} \tag{7}$$

$$\langle Y_1^o\rangle = \frac{1}{\sqrt{4\pi}}\left\{\frac{3.464\ \mathrm{Re}(SP^*) + 6.928\ \mathrm{Re}(PD^*)}{|S|^2 + 3|P|^2 + 5|D|^2}\right\} \tag{8}$$

$$\langle Y_2^o\rangle = \frac{1}{\sqrt{4\pi}}\left\{\frac{2.683|P|^2 + 4.472\ \mathrm{Re}(SD^*) + 3.194|D|^2}{|S|^2 + 3|P|^2 + 5|D|^2}\right\} \tag{9}$$

$$\langle Y_3^o\rangle = \frac{1}{\sqrt{4\pi}}\left\{\frac{6.803\ \mathrm{Re}(PD^*)}{|S|^2 + 3|P|^2 + 5|D|^2}\right\} \tag{10}$$

$$\langle Y_4^o\rangle = \frac{1}{\sqrt{4\pi}}\left\{\frac{4.286|D|^2}{|S|^2 + 3|P|^2 + 5|D|^2}\right\} \tag{11}$$

in which S, P, and D are the complex amplitudes for $K^+\pi^-$ elastic scattering.[19] Initially we neglect the contribution of $I = 3/2$ $K^+\pi^-$ elastic scattering which is known to be small and have no structure from threshold up to $m(K\pi) \sim 2$ GeV.[20] The P and D amplitudes in the above formulas have been parametrized as simple Breit-Wigner forms fixed at conventional values[21] for the $K^*(890)$ and $K^*(1420)$ respectively, i.e.,

$$P \text{ or } D = \frac{x\Gamma/2}{m_o - m - i\Gamma/2} \tag{12}$$

where $m_o = 0.901$ GeV[22] or 1.420 GeV and $\Gamma = 0.050$ GeV or 0.100 GeV for P and D respectively, x is the elasticity which is taken to be 1 and 0.57 for P and D respectively, and m refers to the $K^+\pi^-$ invariant mass.

For the S wave we have taken the simple parametrization,

$$S = \frac{e^{2i\delta^o} - 1}{2i}\ , \tag{13}$$

where δ^o is the phase shift. The parametrization assumes an S-wave elasticity of unity. This assumption can be justified on the following grounds. The

lowest mass systems which can be produced inelastically from a $J^P = 0^+$ $K\pi$ state are $K\pi\pi\pi$ (multi-body) and $K^*(890)\rho(765)$ (quasi-two-body). The latter has a threshold of nearly 1700 MeV. Although the $K\pi\pi\pi$ can be produced at 920 MeV, phase space considerations favor very much higher masses. It is therefore reasonable that in the $K\pi$ mass range below 1.7 GeV, the S wave be assumed to remain essentially elastic.

We have made a series of fits to the values of δ^o as a function of $K\pi$ mass with the following inputs as shown in Table IV. The results are shown in Figs. 7, 8, 9 as indicated in Table IV. A representative fit is shown in Fig. 10.

The $\langle Y_\ell^o \rangle$ are reproduced qualitatively by this model as can be seen from this figure. We have investigated the effect of the $I = 3/2$ $K\pi$ contribution by putting the entire $K^-\pi^-$ cross section determined by Cho et al.[20] into an elastic S wave. The effect, as seen in Fig. 9, is relatively small and therefore does not significantly change any conclusion one might draw from Figs. 7 and 8.

The above model is obviously an oversimplified description of what is going on. Our approach is one of using the minimum set of partial wave amplitudes required to give a qualitative representation of the data. A more precise analysis would have to include (a) amplitudes due to waves with $\ell > 2$, (b) P-wave contributions other than the $K^*(890)$, and (c) a more accurate representation of the D-wave behavior near 1.4 GeV. All these effects which will modify the δ^o values are likely to become most important in the high mass region.

It is well known that there are several kinds of ambiguities in the determination of the phase shifts. First of all any phase shift can be shifted by any multiple of 180°. Secondly, in mass regions where the $K\pi$ cross section is dominated by a single partial wave, the determination of other phase shifts depends principally on interference terms which lead to another type of ambiguity. Thus in the neighborhood of the $K^*(890)$, if δ° is a solution for the S-wave phase shift and δ^1 the P-wave phase shift at the same $m(K\pi)$, then $\overline{\delta^{\circ}}$ defined from,

$$\overline{\delta^{\circ}} \approx \pi/2 - (\delta^{\circ} - \delta^1) \quad , \qquad (14)$$

is also a solution.[2,3] A similar ambiguity occurs in the neighborhood of the $K^*(1420)$. Distributions of χ^2 versus δ° for two $K\pi$ mass bins are shown in Fig. 11 to illustrate the manner in which the ambiguities enter. We have indicated those mass bins where there is a serious ambiguity of the sort shown

in Fig. 10 by dashed crosses in the results of Figs. 7 to 9. In interpreting these figures, it must be remembered that the 180° ambiguity, though not explicitly exhibited, is also there and can be used to form a smoothly varying dependence of δ^o on $m(K\pi)$.

A more explicit representation of the possible solutions is shown in Fig. 12 based on the use of the physical region $\langle Y_\ell^o \rangle$ and the cross-section extrapolation "$t\sigma$" = a + bt. This representation can be characterized as follows:

(i) Between the $K^*(890)$ and the $K^*(1420)$ the S wave appears to have a relatively slow variation, and a large phase shift crossing 90° (or 270°) near $m(K\pi) \approx 1.3$ GeV.

(ii) Near both 0.89 and 1.4 GeV the S wave can either maintain its fairly slow variation or exhibit a very sharp upward rise corresponding to narrow resonances at either or both of these masses. This behavior near 0.89 GeV has been previously observed in analyses of reactions (1) and (2c).[2-4] An S-wave resonance near 1.4 GeV would correspond to the interpretation of part of these data discussed earlier.[7]

Although Fig. 12 uses a particular set of inputs, it is clear from Figs. 7 and 8 that qualitatively similar representations can be made from the other inputs in Table IV.

V. CONCLUSIONS

We have determined $K^+\pi^-$ elastic scattering cross sections and angular distributions for $m(K\pi) < 1.7$ GeV, using the reaction $K^+n \to K^+\pi^-p$ at 12 GeV/c. We have interpreted these data in terms of a simple model for $K\pi$ scattering which consists of the $K^*(890)$ and $K^*(1420)$ resonances using conventional parameters and an elastic $I = 1/2$ S-wave. We find that this model gives a reasonable representation of the gross features of our data. The S-wave phase shift, δ^o, as determined in this analysis has the following characteristics:

(1) For $m(K\pi) < 1$ GeV, δ^o is in qualitative agreement with the results of

earlier analyses involving different reactions.[2-4] In particular, our data also show both "up" and "down" solutions. However, our values for δ^{o} in this mass region for the down solution tend to be somewhat larger than those of Ref. 3.

(2) For $m(K\pi)$ between 1.0 and 1.3 GeV, δ^{o} remains constant at a value of about 90^{o} ("down" solution) or 270^{o} ("up" solution).

(3) For $m(K\pi) \sim 1.4$ GeV, where the cross section is dominated by the D-wave resonance, we find an additional up-down ambiguity.

(4) For $1.4 \text{ GeV} < m(K\pi) < 1.7$ GeV the phase shift increases by 90^{o} ("down" solution) or 270^{o} ("up" solution). In either case, the S-wave amplitude is close to zero for $m(K\pi) \sim 1.7$ GeV.

In summary, our data show that the S-wave amplitude performs at least one complete loop in the Argand plot. For each of the two "up" solutions which may be chosen, an additional narrow resonance loop is introduced in the Argand plot. The two possible additional loops occur in the neighborhoods of the $K^{*}(890)$ and $K^{*}(1420)$.

We wish to thank Eugene Colton and Tom Trippe for many helpful discussions.

We gratefully acknowledge the help of the SLAC accelerator operation group, and in particular we thank J. Murray, R. Gearhart, R. Watt, and the staff of the 82-inch bubble chamber for help with the exposure. We acknowledge the valuable support given by our scanning and programming staff, especially E. R. Burns, A. P. Habegger, and H. White and the staff of the Flying-Spot Digitizer.

FOOTNOTES AND REFERENCES

†Work supported by the U. S. Atomic Energy Commission.

*Present address: Department of Physics, California Institute of Technology, Pasadena, California 91109.

1. T. Trippe et al., Phys. Lett. 28B, 203 (1968).
2. R. Mercer et al., Nucl. Phys. B32, 381 (1971).
3. H.H. Bingham et al., CERN preprint CERN/D.Ph.II/Phys. 71-22 Rev (1971).
4. H. Yuta et al., Phys. Rev. Lett. 26, 1502 (1971).
5. A. Firestone, G. Goldhaber, A. Hirata, D. Lissauer, and G. H. Trilling, Phys. Rev. Lett. 25, 958 (1970).
6. A. Firestone, G. Goldhaber, and D. Lissauer, Lawrence Radiation Laboratory Report UCRL-20076 (1970), unpublished.
7. A. Firestone, G. Goldhaber, and D. Lissauer, Phys. Rev. Lett. 26, 1460 (1971).
8. A. Firestone, G. Goldhaber, D. Lissauer, and G. H. Trilling, Phys. Lett. 36B, 513 (1971).
9. In fact, since the Fermi momentum of the neutron in the deuteron is in general unknown, t is defined to be the square of the four-momentum transfer from the incident K^+ to the outgoing $(K^+\pi^-)$ system. The sign of t is taken to be positive in the physical region.
10. Eugene Colton and Ernest Malamud, Phys. Rev. D3, 2033 (1971).
11. Z. Ming Ma et al., Phys. Rev. Lett. 23, 342 (1969).
12. See, for example, E. Ferrari and F. Selleri, Nuovo Cimento Suppl. 24, 453 (1962).
13. H. P. Dürr and H. Pilkuhn, Nuovo Cimento 40, 899 (1965).
14. G. Goldhaber et al., Phys. Lett. 6, 62 (1963).
15. G. Wolf, Phys. Rev. Lett. 19, 925 (1967).
16. P. Schlein in Proceedings of the Conference on $\pi\pi$ and $K\pi$ Interactions

(Argonne National Laboratory, Argonne, Illinois, 1969), pp. 1 and 446; see also a review talk by P. Schlein, in Meson Spectroscopy, edited by C. Baltay and A. H. Rosenfeld (W. A. Benjamin, New York, 1968), p. 161.

17. G. L. Kane in Experimental Meson Spectroscopy, edited by C. Baltay and A. H. Rosenfeld (Columbia University, New York, 1970), p. 1.

18. This interpretation is completely consistent with the results of our "$t\sigma$" = bt fit; the "$t\sigma$" = a + bt fit gives a somewhat higher cross section than even the sum of the S and P wave unitarity limits.

19. See for example T. Trippe, Ph.D. thesis, University of California at Los Angeles (unpublished).

20. Y. Cho et al., Phys. Lett. 32B, 409 (1971).

21. Particle Data Group, Rev. Mod. Phys. 43, 51 (1971).

22. We have used $M(K^{*o})$ as obtained from the values of $M(K^{*\pm})$ and $M(K^{*o}) - M(K^{*\pm}) = 8\pm3$ MeV quoted in Ref. 21. A more precise recent value for $M(K^{*o}) - M(K^{*-}) = 5.7\pm1.7$ MeV by Aguilar-Benitez et al. (BNL preprint, 1971, submitted to Phys. Rev.) was not included in the above average.

Table I. $\sigma(K^+\pi^- \rightarrow K^+\pi^-)$ from extrapolation of "$t\sigma$".

		"$t\sigma$" = bt		"$t\sigma$" = a + bt			
$M(K^+\pi^-)$ (GeV)	Events	$\frac{\chi^2}{9 \text{ dof}}$	$b=\sigma$ (mb)	$\frac{\chi^2}{8 \text{ dof}}$	a (mb(GeV/c)^2)	b (mb)	σ (mb)
0.70-0.80	30	5.9	12.1±2.8	4.8	-0.07±0.07	15.3±4.1	19.0±5.4
0.80-0.84	34	6.1	26.1±5.2	5.8	-0.08±0.16	29.4±8.4	33.4±11.6
0.84-0.88	109	31.7	46.1±5.7	25.9	-0.36±0.15	63.2±9.1	81.9±12.0
0.88-0.92	203	19.6	89.0±7.2	9.8	-0.60±0.19	116.3±11.3	146.9±14.9
0.92-0.96	90	23.9	27.0±3.5	23.8	-0.02±0.10	27.6±5.0	28.5±7.1
0.96-1.00	53	15.0	11.6±2.0	10.4	-0.10±0.05	16.7±3.1	22.0±4.0
1.00-1.10	138	6.3	13.4±1.2	4.8	-0.04±0.03	14.9±1.7	17.2±2.5
1.10-1.20	127	9.5	8.7±0.8	9.2	0.01±0.03	8.3±1.1	7.5±1.8
1.20-1.30	174	18.7	8.2±0.7	12.4	-0.05±0.02	10.0±1.0	12.3±1.4
1.30-1.35	131	24.5	9.2±0.9	22.3	-0.04±0.02	10.6±1.3	12.5±1.8
1.35-1.40	171	4.9	13.4±1.1	4.7	-0.02±0.03	13.9±1.5	14.8±2.3
1.40-1.45	181	14.6	12.1±1.0	14.3	-0.02±0.03	12.6±1.3	13.5±2.2
1.45-1.50	127	13.5	7.1±0.7	6.4	-0.05±0.02	9.0±1.0	11.7±1.4
1.50-1.60	154	17.9	3.9±0.3	17.8	0.00±0.01	4.0±0.5	4.2±0.8
1.60-1.70	165	6.0	3.9±0.3	3.8	0.05±0.03	3.1±0.6	0.6±1.8
1.70-1.75	99	14.2	3.5±0.4	6.8	-0.04±0.02	4.6±0.6	6.5±0.9
1.75-1.80	100	12.2	3.4±0.4	12.2	0.00±0.02	3.3±0.6	3.3±1.3
1.80-1.85	92	14.4	2.9±0.3	14.1	-0.02±0.03	3.2±0.7	4.1±1.8
1.85-1.90	102	6.8	3.3±0.3	6.2	-0.03±0.03	3.8±0.7	5.3±1.9
1.90-1.95	112	10.2	3.5±0.4	6.2	-0.07±0.03	4.8±0.7	8.3±1.9
1.95-2.00	88	10.0	2.6±0.3	9.6	-0.02±0.03	3.0±0.6	4.1±1.9

Table II. Extrapolated values of $\langle Y_\ell^o \rangle$.

$M(K^+\pi^-)$ GeV	$\langle Y_1^o \rangle$	$\langle Y_2^o \rangle$	$\langle Y_3^o \rangle$	$\langle Y_4^o \rangle$
0.70-0.80	0.21±0.04	-0.09±0.07	0.04±0.08	0.07±0.11
0.80-0.84	0.31±0.11	0.11±0.10	0.04±0.11	0.09±0.11
0.84-0.88	0.16±0.06	0.15±0.06	0.03±0.06	0.09±0.06
0.88-0.92	0.24±0.04	0.22±0.04	0.06±0.05	0.07±0.04
0.92-0.96	0.05±0.06	0.10±0.06	0.13±0.06	-0.07±0.06
0.96-1.00	-0.12±0.08	-0.02±0.08	0.11±0.08	0.04±0.08
1.00-1.10	0.01±0.05	-0.01±0.05	0.05±0.04	0.07±0.05
1.10-1.20	0.12±0.05	0.10±0.05	0.11±0.05	0.08±0.05
1.20-1.30	0.14±0.05	0.06±0.05	-0.02±0.05	0.08±0.05
1.30-1.35	-0.06±0.06	0.09±0.06	-0.03±0.05	-0.05±0.06
1.35-1.40	-0.02±0.05	0.14±0.05	0.08±0.05	0.02±0.05
1.40-1.45	-0.06±0.06	0.30±0.05	-0.01±0.06	0.19±0.05
1.45-1.50	-0.15±0.08	0.35±0.07	-0.08±0.08	0.07±0.07
1.50-1.60	-0.05±0.07	0.40±0.06	0.02±0.07	0.26±0.06
1.60-1.70	0.10±0.06	0.28±0.05	0.01±0.07	0.26±0.06
1.70-1.75	0.26±0.08	0.22±0.07	0.21±0.07	0.01±0.09
1.75-1.80	0.25±0.07	0.32±0.08	0.26±0.08	0.11±0.09
1.80-1.85	0.37±0.09	0.40±0.09	0.31±0.09	0.16±0.09
1.85-1.90	0.25±0.08	0.30±0.07	0.27±0.07	0.11±0.08
1.90-1.95	0.28±0.09	0.35±0.09	0.43±0.10	0.13±0.10
1.95-2.00	0.27±0.10	0.46±0.11	0.46±0.10	0.36±0.10

Table III. Values of $\langle Y_\ell^0 \rangle$ in the physical region [$t < 0.2$ (GeV/c)^2].

$M(K^+\pi^-)$ GeV	$\langle Y_1^0 \rangle$	$\langle Y_2^0 \rangle$	$\langle Y_3^0 \rangle$	$\langle Y_4^0 \rangle$
0.70-0.80	0.192±0.037	0.025±0.049	0.008±0.047	0.004±0.041
0.80-0.84	0.232±0.036	0.102±0.046	0.027±0.050	-0.014±0.047
0.84-0.88	0.147±0.027	0.106±0.028	0.004±0.030	0.012±0.030
0.88-0.92	0.105±0.022	0.135±0.021	-0.006±0.022	0.028±0.022
0.92-0.96	0.017±0.035	0.099±0.030	0.033±0.033	-0.040±0.032
0.96-1.00	-0.038±0.044	0.091±0.044	0.007±0.045	0.062±0.045
1.00-1.10	-0.034±0.025	0.029±0.025	-0.020±0.026	0.009±0.027
1.10-1.20	0.015±0.027	0.062±0.028	0.059±0.028	0.038±0.028
1.20-1.30	-0.020±0.015	0.075±0.023	-0.009±0.025	0.026±0.024
1.30-1.35	0.052±0.029	0.116±0.028	0.018±0.030	0.057±0.029
1.35-1.40	0.071±0.025	0.111±0.023	0.053±0.023	0.005±0.024
1.40-1.45	0.022±0.027	0.243±0.021	-0.023±0.026	0.098±0.025
1.45-1.50	0.008±0.034	0.311±0.024	0.010±0.035	0.150±0.032
1.50-1.60	0.116±0.030	0.342±0.020	0.105±0.032	0.174±0.031
1.60-1.70	0.167±0.027	0.278±0.022	0.085±0.030	0.140±0.029
1.70-1.75	0.244±0.030	0.282±0.026	0.200±0.032	0.078±0.037
1.75-1.80	0.239±0.030	0.316±0.027	0.255±0.033	0.172±0.037
1.80-1.85	0.232±0.031	0.286±0.029	0.298±0.029	0.144±0.040
1.85-1.90	0.263±0.029	0.324±0.024	0.286±0.028	0.128±0.038
1.90-1.95	0.294±0.027	0.356±0.023	0.332±0.027	0.191±0.037
1.95-2.00	0.350±0.024	0.400±0.023	0.351±0.031	0.253±0.039

Table IV. Information used in phase-shift calculation.

$\langle Y_\ell^0 \rangle$	Kπ cross-section information used	I = 3/2 contribution	Figure no. of results
Extrapolated	None	Neglected	7a
Extrapolated	"tσ" = a + bt	Neglected	7b
Extrapolated	"tσ" = bt	Neglected	7c
Physical Region	None	Neglected	8a
Physical Region	"tσ" = a + bt	Neglected	8b
Physical Region	"tσ" = bt	Neglected	8c, 12
Physical Region	"tσ" = bt	Included as S wave	9

FIGURE CAPTIONS

Fig. 1. Kinematic boundaries for the two reactions $K^+p \rightarrow K^+\pi^-\Delta^{++}$ (curve a) and $K^+n \rightarrow K^+\pi^-p$ (curve b) evaluated at an incident momentum of 12 GeV/c.

Fig. 2. Extrapolated cross section $\sigma(K^+\pi^- \rightarrow K^+\pi^-)$ using the extrapolation "$t\sigma$" = bt. The three labeled curves represent the P-wave unitarity limit, the S-wave unitarity limit and the D-wave unitarity limit. Curve D is calculated assuming a D-wave elasticity of 57%.

Fig. 3. Extrapolated cross section $\sigma(K^+\pi^- \rightarrow K^+\pi^-)$ using the extrapolation "$t\sigma$" = a + bt. The curves are the same as in Fig. 2.

Fig. 4. The extrapolation to the pion pole, "$t\sigma$" = a + bt in each of the 21 mass bins.

Fig. 5. The extrapolated values of the spherical harmonics, (a) $\langle Y_1^0 \rangle$, (b) $\langle Y_2^0 \rangle$, (c) $\langle Y_3^0 \rangle$, and (d) $\langle Y_4^0 \rangle$.

Fig. 6. Spherical harmonics in the physical region for events with $t < 0.2$ $(GeV/c)^2$. (a) $\langle Y_1^0 \rangle$, (b) $\langle Y_2^0 \rangle$, (c) $\langle Y_3^0 \rangle$, and (d) $\langle Y_4^0 \rangle$ (not extrapolated).

Fig. 7. The S-wave phase shift, δ^0, as a function of $m(K\pi)$ for the fits with extrapolated values of the spherical harmonics for (a) no cross-section data used, (b) the cross-section data from the extrapolation "$t\sigma$" = a + bt used, and (c) the cross-section data from the extrapolation "$t\sigma$" = bt used. The dashed crosses correspond to explicitly ambiguous solutions.

Fig. 8. The S-wave phase shift, δ^0, as a function of $m(K\pi)$ for the fit with spherical harmonics evaluated in the physical region and (a) no cross-section data used, (b) the cross-section data from the extrapolation "$t\sigma$" = a + bt used, and (c) the cross-section data from the extrapolation "$t\sigma$" = bt used. The dashed crosses correspond to explicitly ambiguous solutions.

Fig. 9. The S-wave phase shift, δ^0, as a function of $m(K\pi)$ for the fits using spherical harmonics evaluated in the physical region, cross-section data

from extrapolation "tσ" = bt, I = 3/2 contribution to Kπ elastic scattering put in explicitly.

Fig. 10. The spherical harmonics in the physical region for events with $t < 0.2$ $(GeV/c)^2$ (same as in Fig. 6). The curves are the results of fits to the data carried out to determine δ^o, as in Fig. 8c; i.e., for "tσ" = bt.

Fig. 11. Chisquare of the fit to δ^o as a function of the S-wave phase shift δ^o in mass bins (a) 0.88 GeV < m(Kπ) < 0.92 GeV, and (b) 1.40 GeV < m(Kπ) < 1.45 GeV. Here again the case corresponding to Fig. 8c is shown; i.e., spherical harmonics in the physical region and "tσ" = bt.

Fig. 12. The S-wave phase shift δ^o vs m(Kπ) again corresponding to the case in Fig. 8c. The four ambiguous solutions are shown explicitly here. The curves are given only to guide the eye.

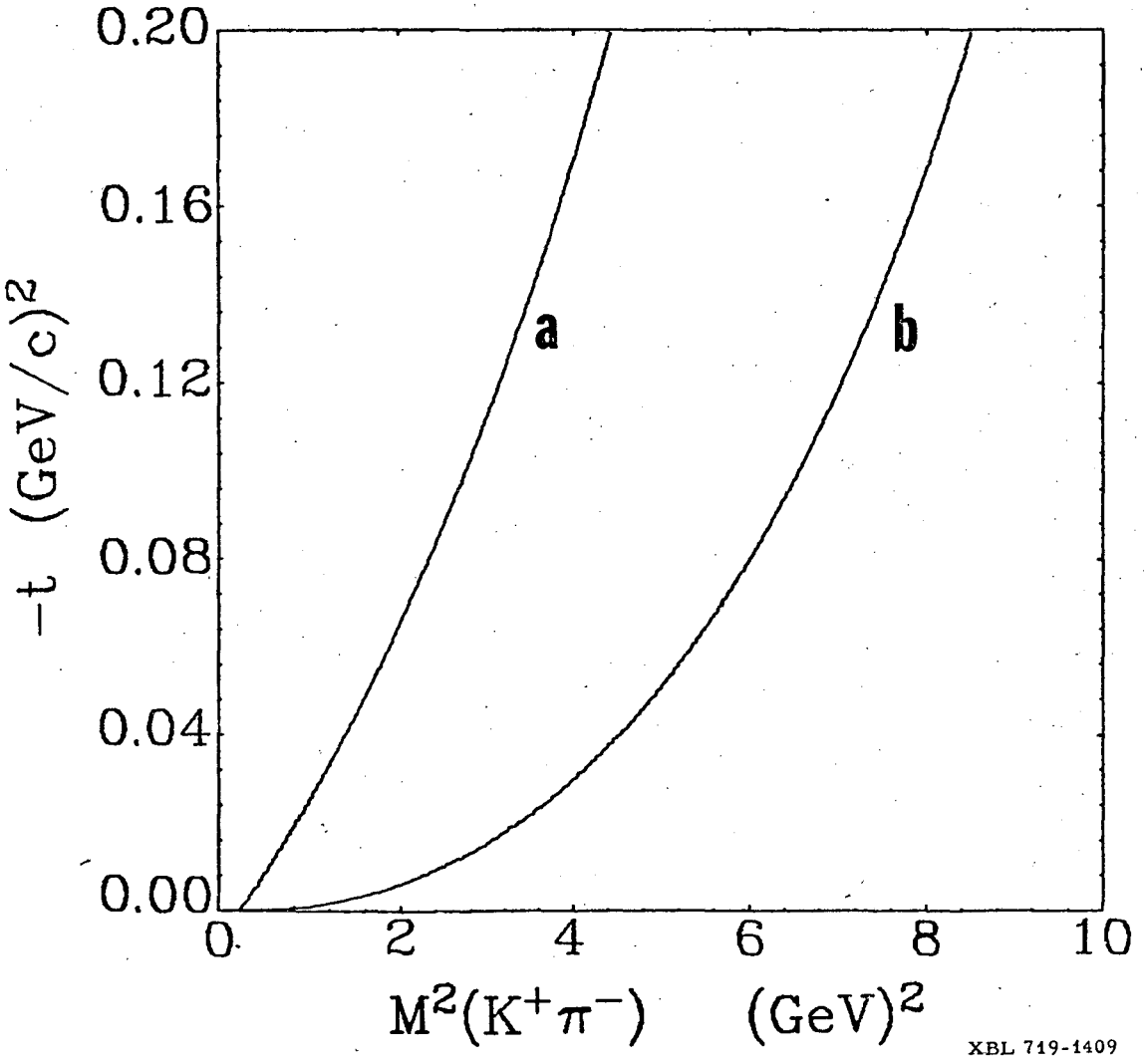
0.20
0.16
0.12
0.08
0.04
0.00
$-t$ $(GeV/c)^2$
a
b
0
2
4
6
8
10
$M^2(K^+\pi^-)$ $(GeV)^2$
XBL 719-1409

Fig. 1

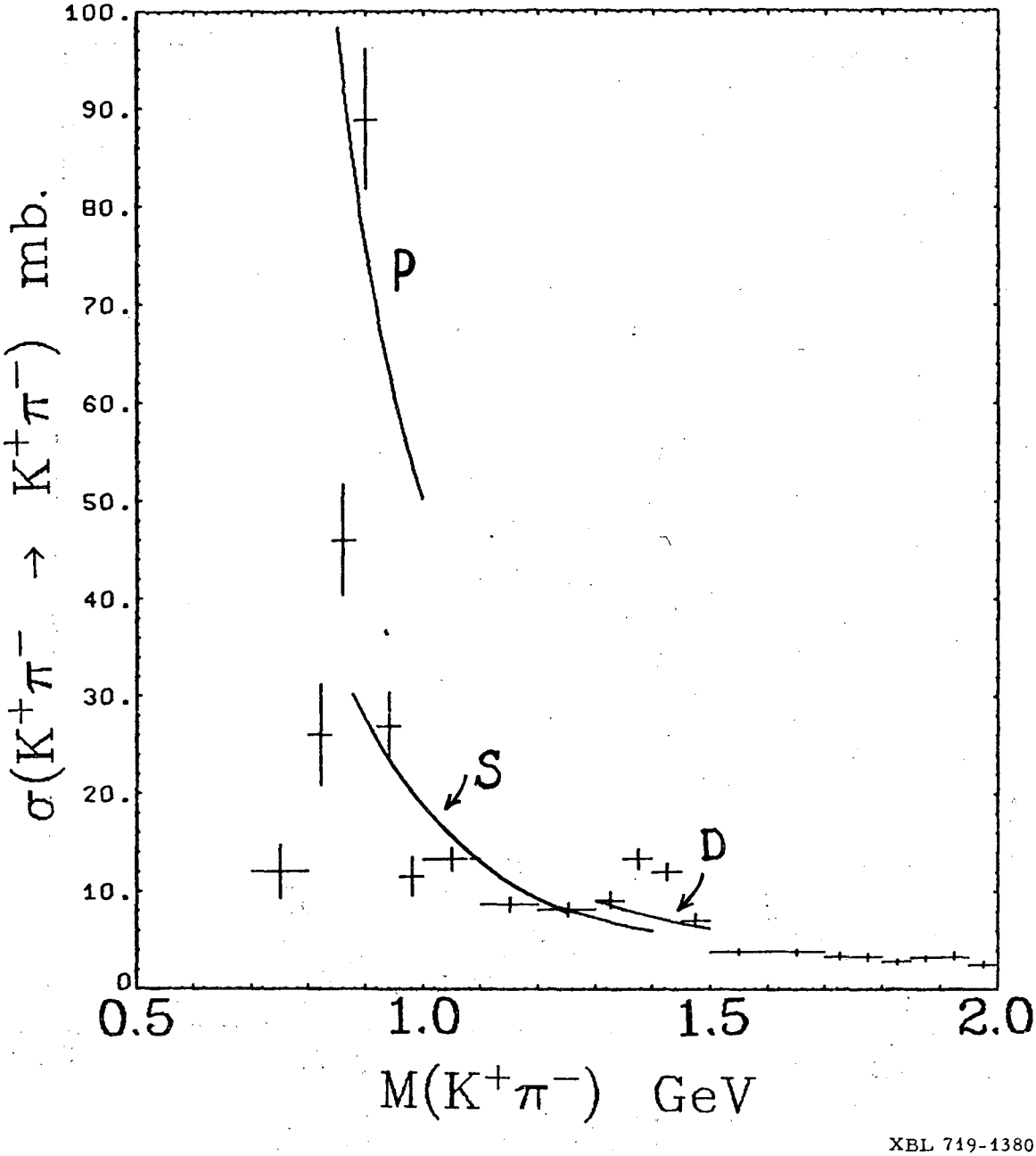

XBL 719-1380

Fig. 2

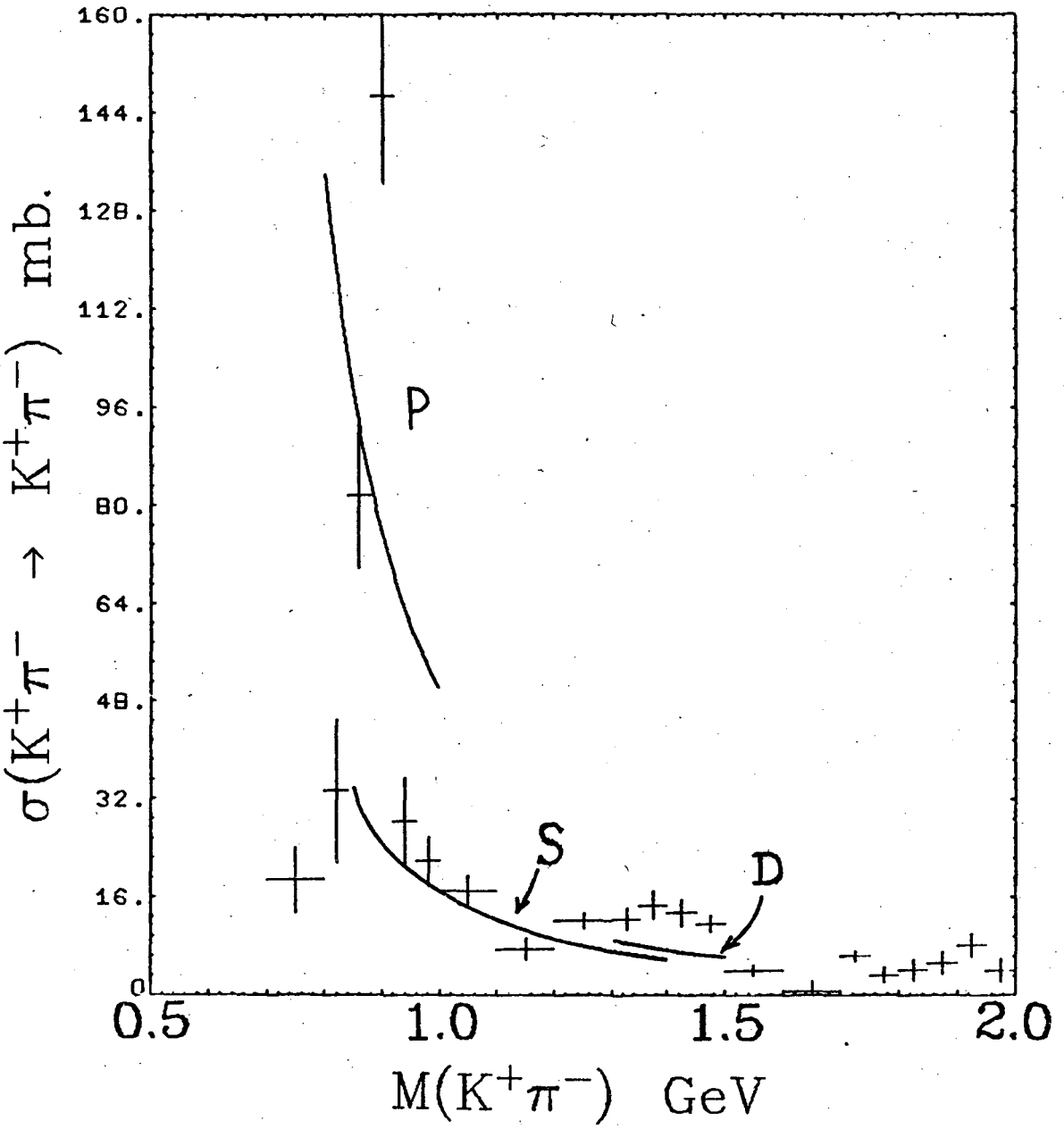

XBL 719-1381

Fig. 3

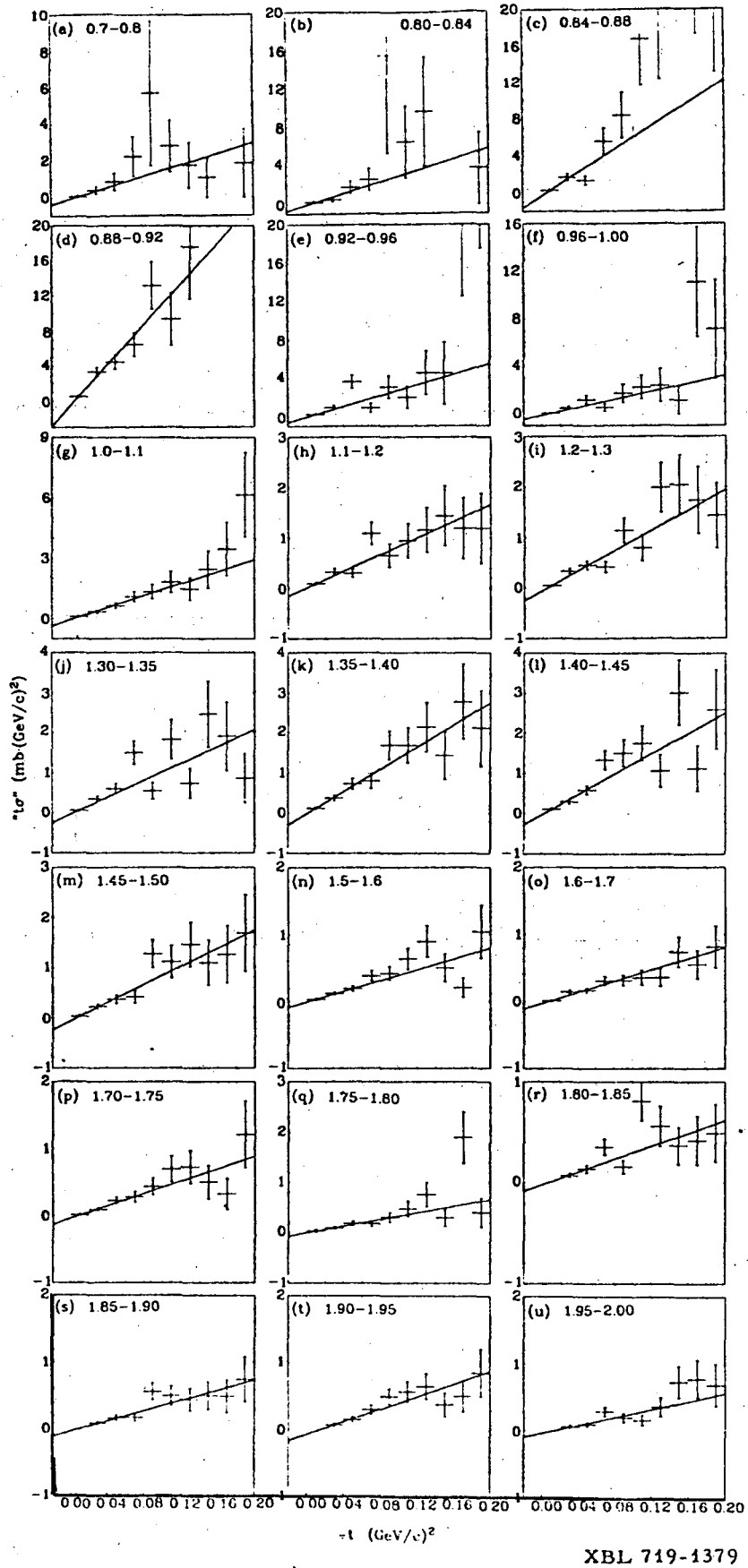

XBL 719-1379

Fig. 4

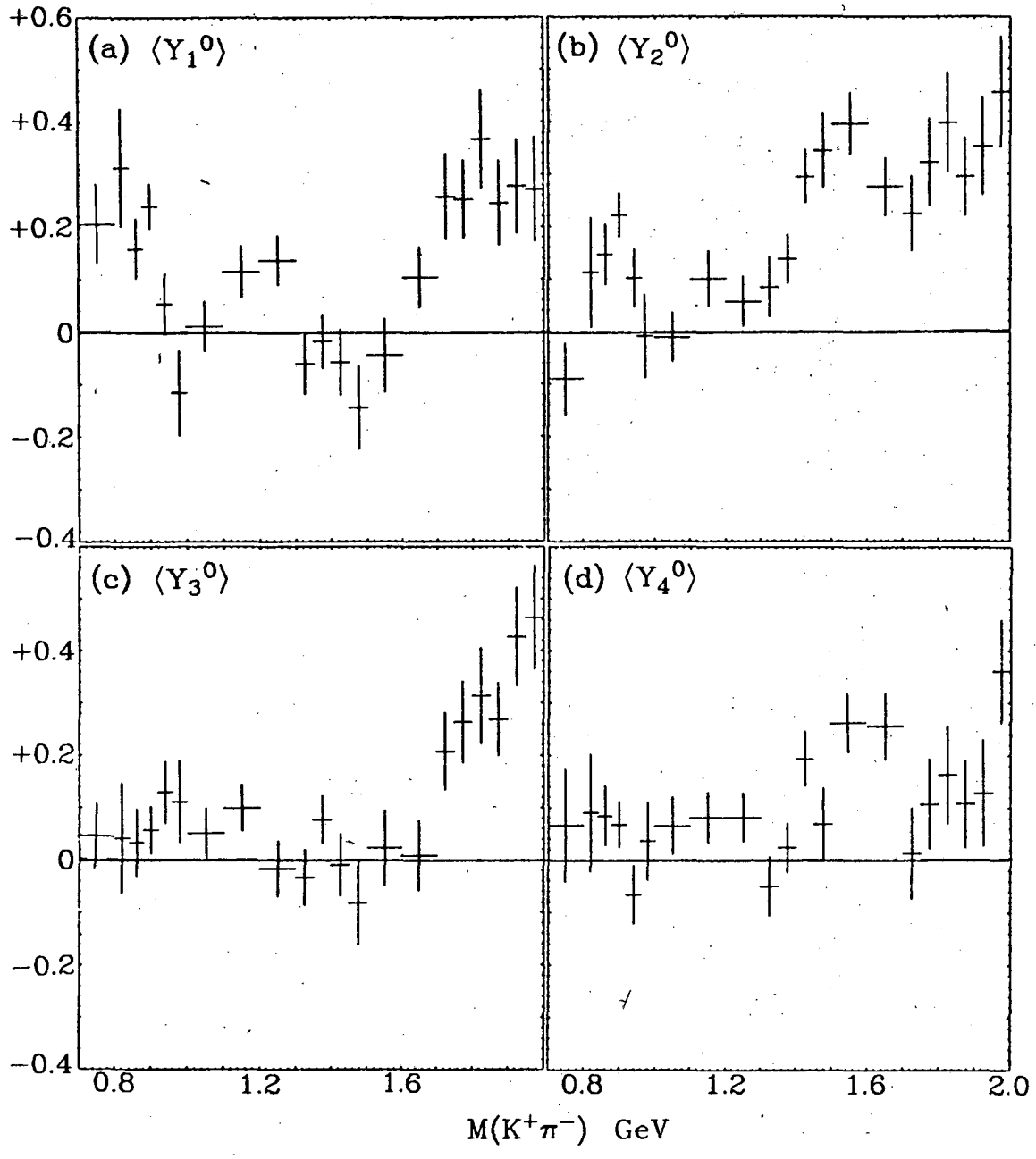
(a) ⟨Y1⁰⟩
(b) ⟨Y2⁰⟩
(c) ⟨Y3⁰⟩
(d) ⟨Y4⁰⟩
+0.6
+0.4
+0.2
0
−0.2
−0.4
0.8
1.2
1.6
2.0
M(K⁺π⁻) GeV
XBL 719-1465

Fig. 5

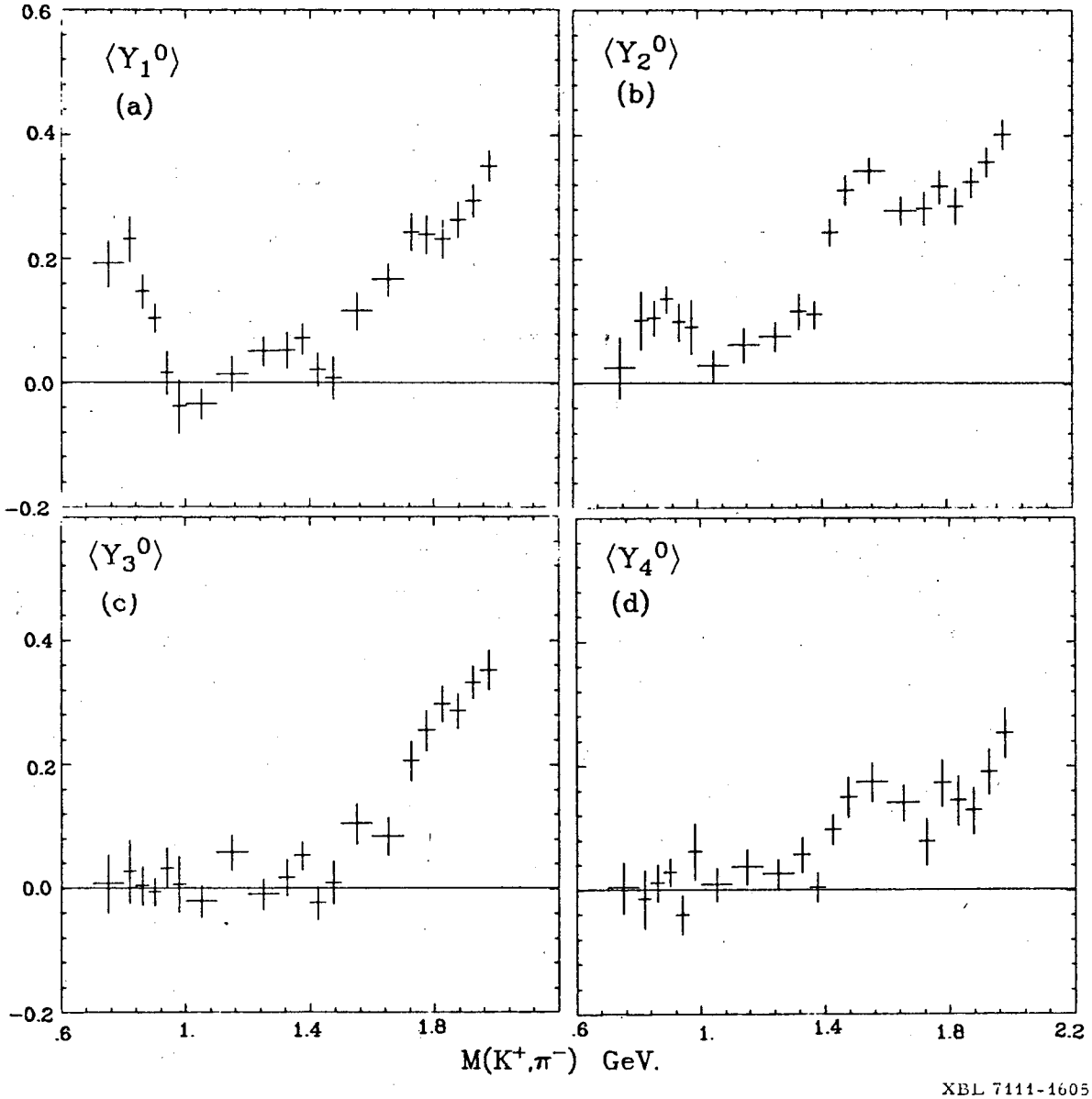

Fig. 6

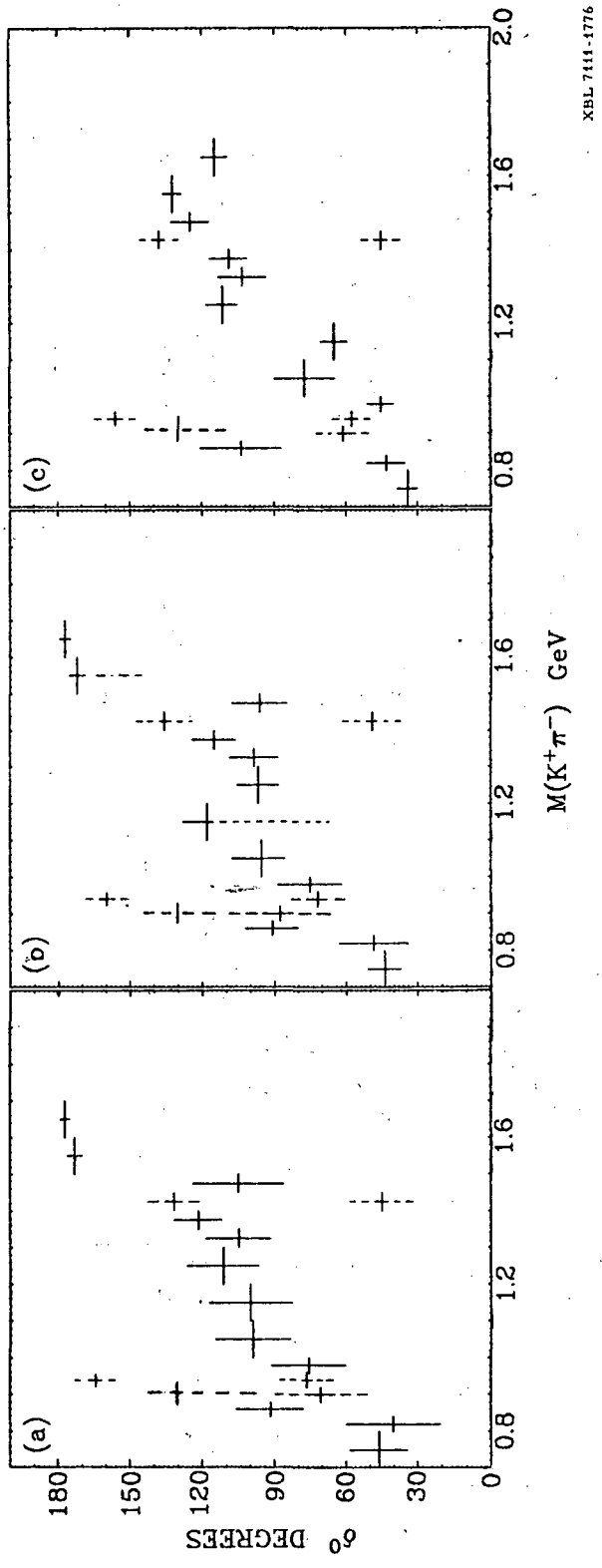
(a)
(b)
(c)
180
150
120
90
60
30
0
0.8
1.2
1.6
2.0
δ^0 DEGREES
$M(K^+\pi^-)$ GeV
XBL 7111-1776

Fig. 7

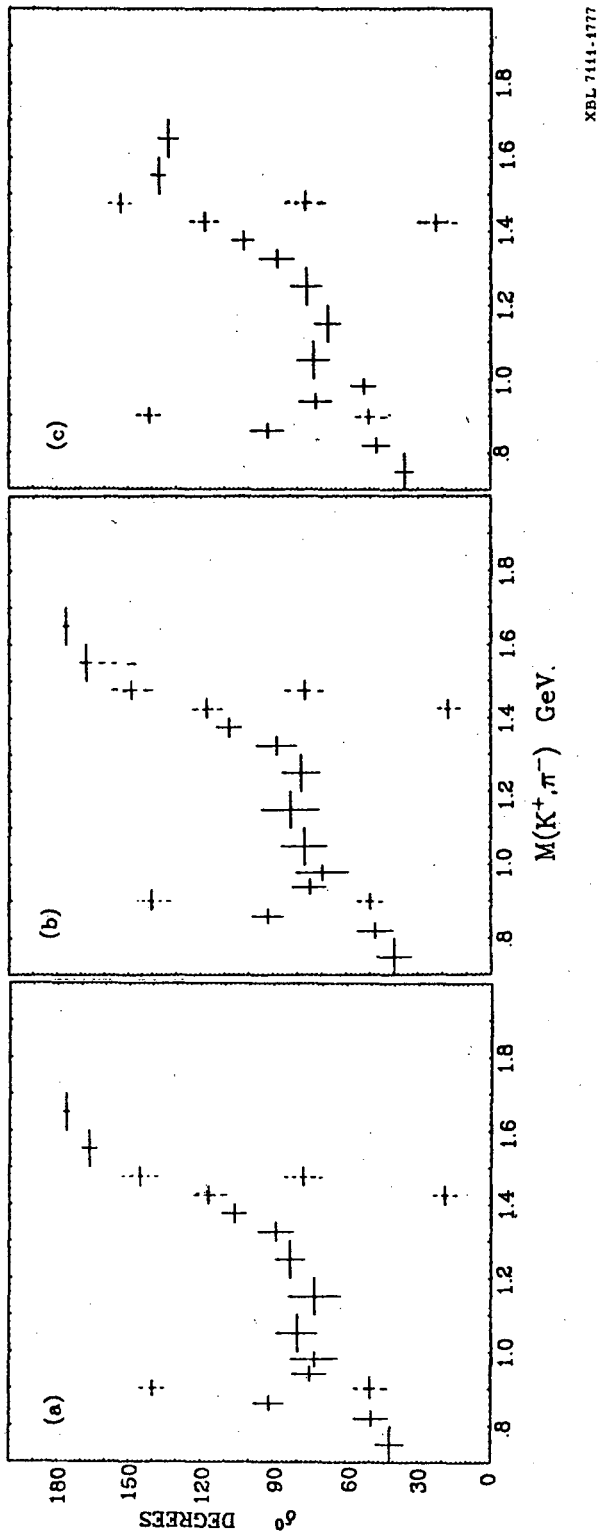
(a)
(b)
(c)
δ° DEGREES
180
150
120
90
60
30
0
.8
1.0
1.2
1.4
1.6
1.8
M(K⁺,π⁻) GeV.
XBL 7111-1777

Fig. 8

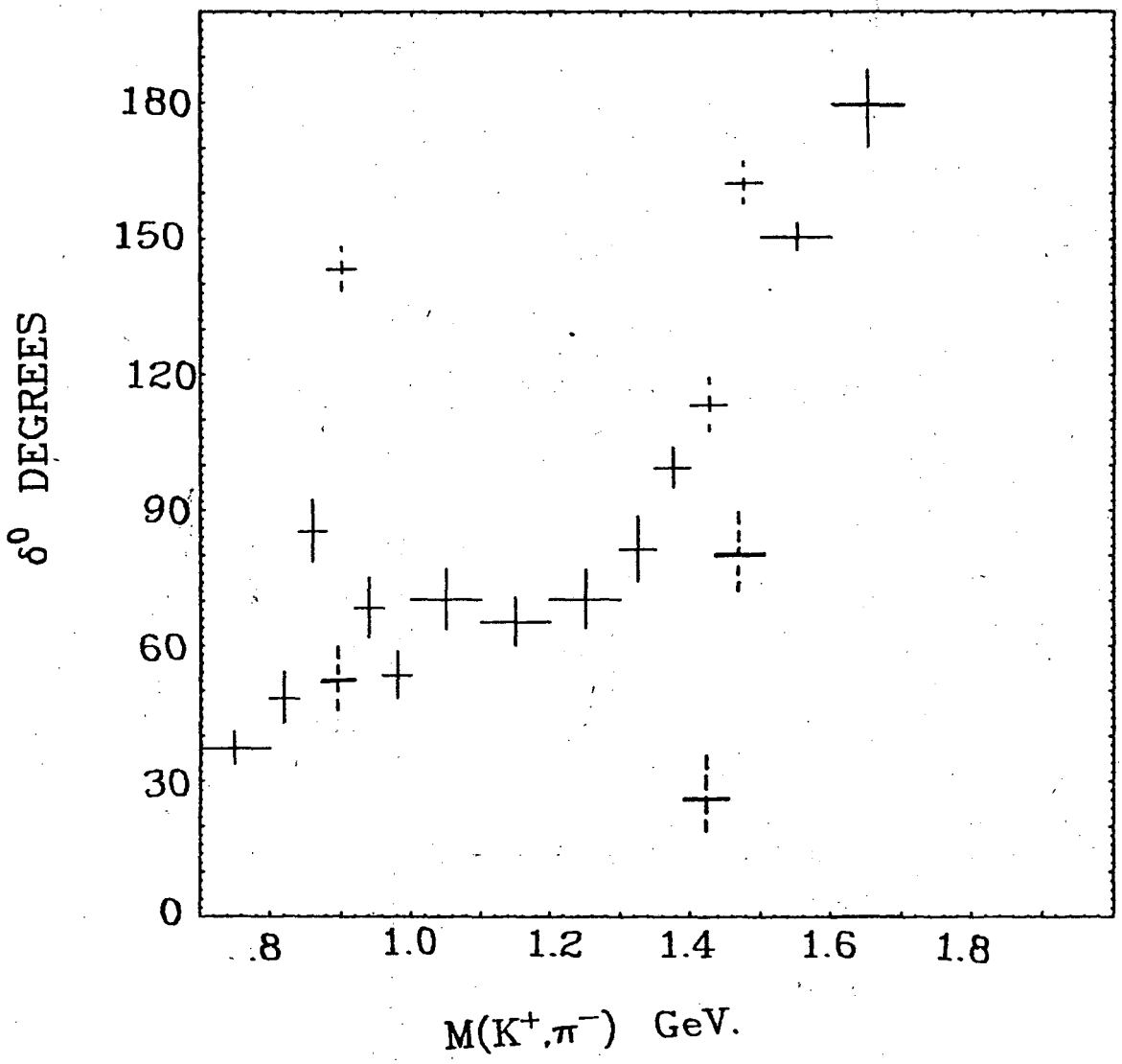
180
150
120
90
60
30
0
δ⁰ DEGREES
.8
1.0
1.2
1.4
1.6
1.8
M(K⁺,π⁻) GeV.
XBL 7111-1779

Fig. 9

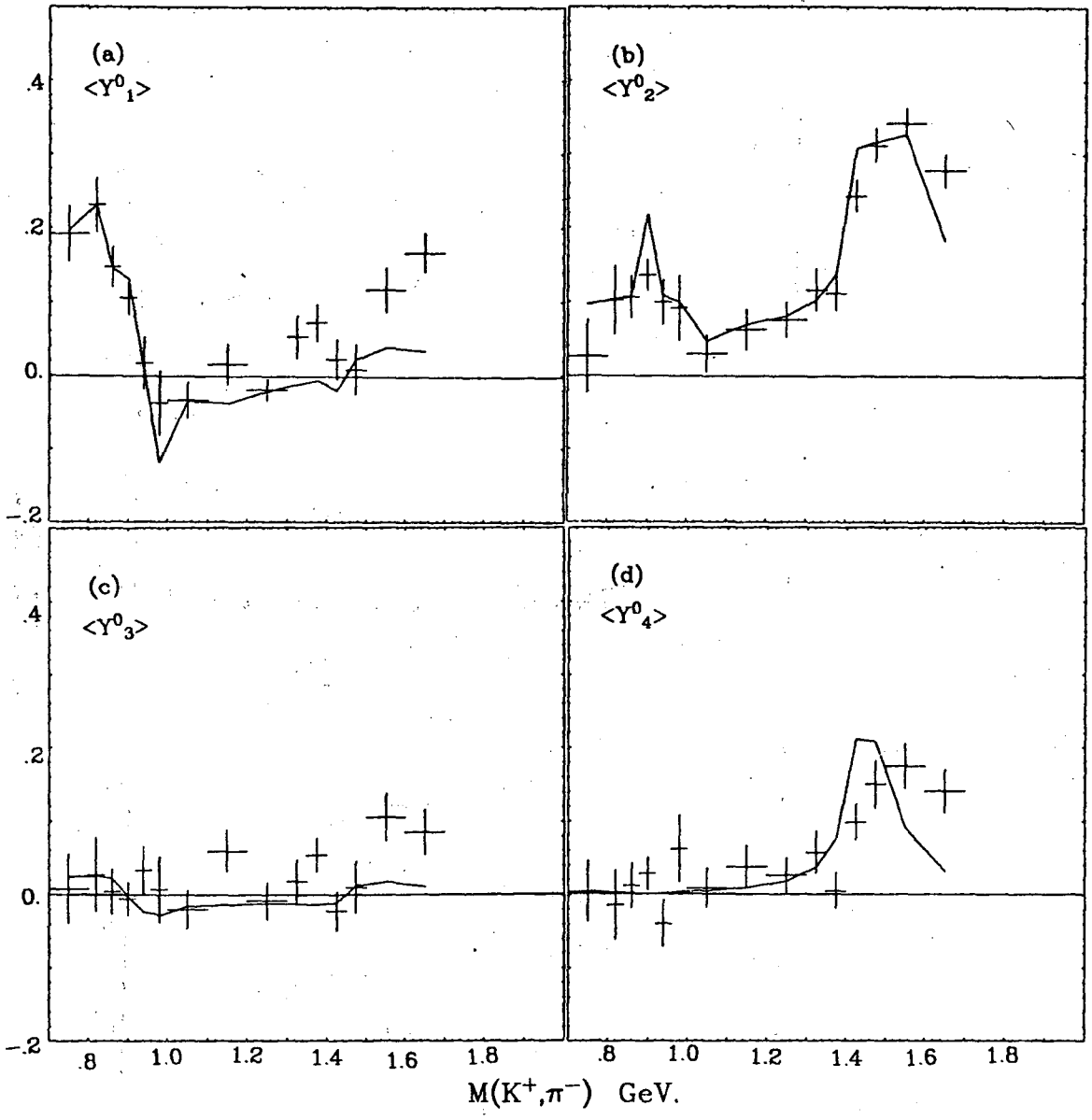

XBL 7111-1778

Fig. 10

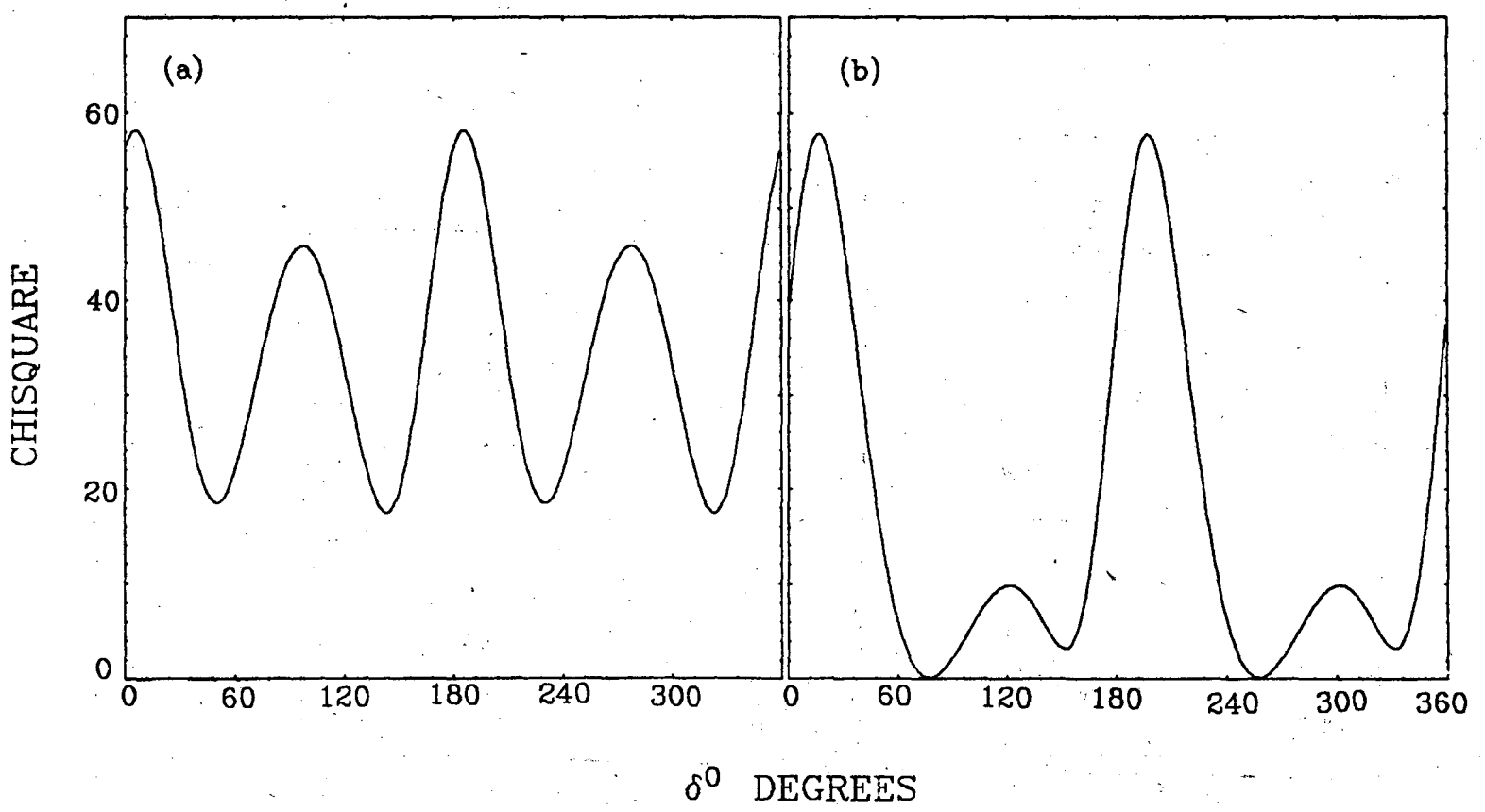

XBL 7111-1774

Fig. 11

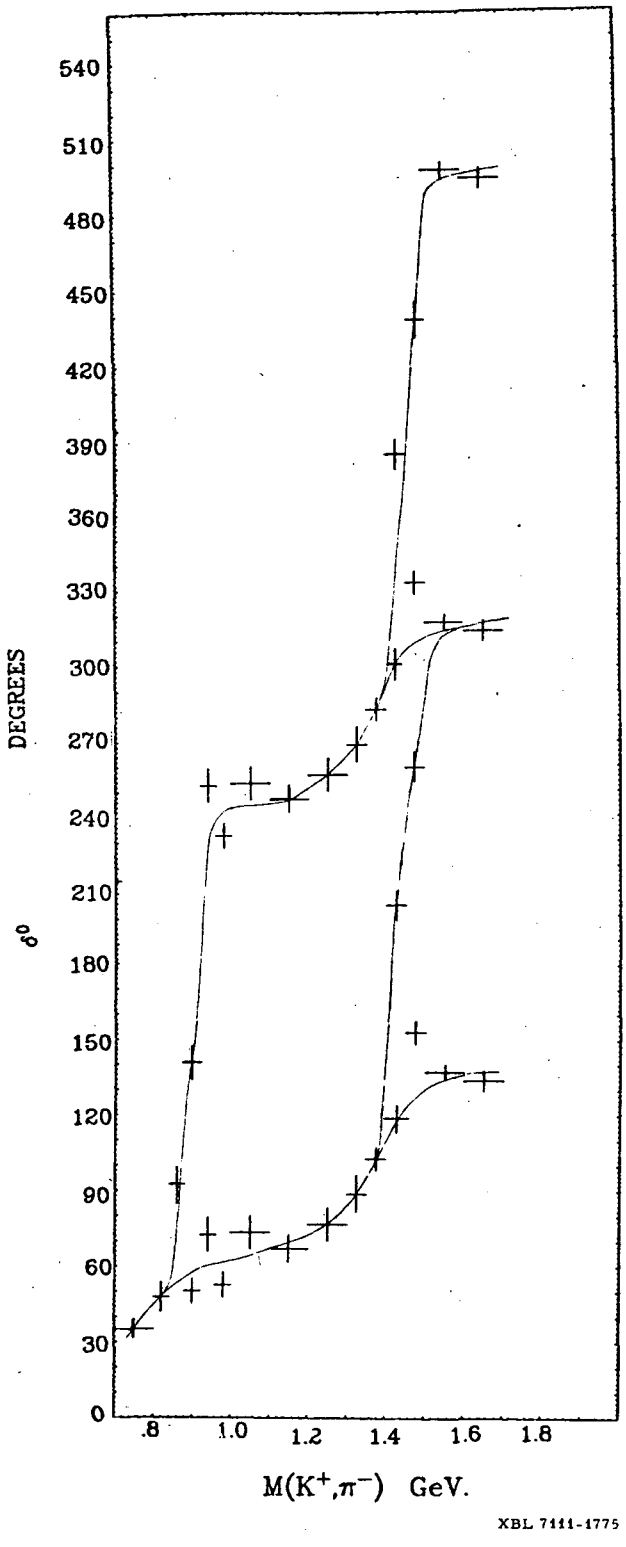

Fig. 12

TECHNICAL INFORMATION DIVISION
LAWRENCE BERKELEY LABORATORY
UNIVERSITY OF CALIFORNIA
BERKELEY, CALIFORNIA 94720